

Simplified Reaction Mechanism for CFD Simulation of Rocket Re-Entry

&Weiran Li¹, &Sihan Di¹, Nanjia Yu^{1*}

&These authors contributed equally to this work and should be considered co-first authors

¹ School of Astronautics, Beihang University

Beijing, China

liweiran@buaa.edu.cn; dsh@buaa.edu.cn; ynjtougao@126.com

Abstract - The chemical environment and flow characteristics during rocket re-entry are highly complex. To improve the computational efficiency of CFD simulations, a simplified reaction mechanism for the rocket re-entry CFD has been developed. Based on the Principal Component Analysis (PCA), the detailed reaction mechanism was simplified, resulting in a mechanism comprising 25 species and 34 reactions. Then the NSGA-III optimization framework was used to optimize the s25r34 mechanism. Comparison of simplified and detailed mechanisms shows that the ignition delay error of the simplified mechanism does not exceed 25%. And the temporal variation trends of three key species remain consistent with the detailed mechanism in both numerical values and trends. The errors introduced during the simplification and optimization processes are within an acceptable range. This simplified reaction mechanism can significantly improve computational efficiency while maintaining reasonable accuracy, serving a reference for CFD simulations of the rocket re-entry process.

Keywords: Mechanism Simplification; Rocket re-entry; CFD; Methane; Combustion

1. Introduction

Rocket re-entry technology is a critical aspect of reusable launch vehicles^[1]. During the descent of a reusable vertically reentering rocket, its external shell is immersed in an intense, unstable thermal gas layer, where the chemical environment is highly complex^{[2]-[3]}. The re-entry process involves intense heat release and intricate flow dynamics, including multiscale turbulence. Understanding the chemical reactions occurring in this process is essential for ensuring the safety of rocket re-entry.

With advancements in CFD (Computational Fluid Dynamics) and increasing computational power, it is now possible to simulate reactive flows numerically. However, stiff reaction equations and a large number of chemical species pose significant computational challenges. To address this, reaction mechanism simplification is often used to reduce computational complexity while maintaining accuracy^[4]. Although simplified mechanisms significantly reduce computational resource demands, errors are bound to be introduced. By optimizing reaction rate adjustments using the error between the simplified and detailed mechanism simulations, a more accurate simplified mechanism can be obtained.

Extensive research has been conducted on combustion processes inside rocket engines, leading to the development of high-precision simplified mechanisms and simplification methods^[5]. However, less attention has been given to the interaction between exhaust gases and air after exiting the nozzle. This study focuses on CFD simulation of methane-oxygen rocket re-entry, proposing a simplified reaction mechanism based on Principal Component Analysis (PCA) and NSGA-III (Non-dominated Sorting Genetic Algorithm III). The developed mechanism significantly reduces computational costs and provides a valuable reference for the numerical simulation of the rocket re-entry process.

2. Method

2.1. Mechanism Simplification Based on PCA

Before applying PCA for mechanism simplification, certain key species are predefined manually. At each time step during ignition simulation, the influence of reaction rates on key species can be represented using a sensitivity matrix

$$S_i = \left(\frac{k_j}{y_k} \frac{\partial y_k}{\partial k_j} \right)_i = \left(\frac{\partial \ln y_k}{\partial \ln k_j} \right)_i \quad (1)$$

where k_j is the reaction rate constant of the j -th reaction, and y_k is the concentration of the k -th important component. To further quantify the influence of reactions on key species, a function is constructed as

$$Q(\mathbf{k}) = \left\| \frac{y_{ki}(\mathbf{k}) - y_{ki}(\mathbf{k}^0)}{y_{ki}(\mathbf{k}^0)} \right\|_2^2 \quad (2)$$

where \mathbf{k} represents the perturbed reaction rate constant vector, and \mathbf{k}^0 denotes the original reaction rate constant.

Using Taylor series expansion, considering that $Q(\mathbf{k}^0) = 0$, and \mathbf{k}^0 is the minimum point of the function,

$$Q(\mathbf{k}) \approx \frac{1}{2} (\Delta \mathbf{k})^T \mathbf{H}(\mathbf{k}^0) \Delta \mathbf{k} \quad (3)$$

where \mathbf{G} is the gradient vector, and \mathbf{H} is the Hessian matrix.

According to reference [6]

$$Q(\mathbf{k}) \approx \hat{Q}(\mathbf{k}) = (\Delta \mathbf{k})^T \mathbf{S}^T \mathbf{S} \Delta \mathbf{k} \quad (4)$$

where \mathbf{S} is the sensitivity matrix. Performing spectral decomposition on $\mathbf{S}^T \mathbf{S}$, the principal component is defined as $\Psi = \mathbf{U}^T \mathbf{k}$, where \mathbf{U} is an orthogonal matrix composed of normalized eigenvectors. Thus, the function can be expressed as

$$\hat{Q}(\mathbf{k}) = \sum_{m=1}^{n_{rr}} \lambda_m \|\Delta \Psi_m\|_2^2 \quad (5)$$

where λ_m is the m -th eigenvector of $\mathbf{S}^T \mathbf{S}$. At this moment, reactions corresponding to larger components in the eigenvectors associated with larger eigenvalues have a greater influence on the key species. Therefore, during the simplification process, these significant reactions should be retained. The PCA-based mechanism simplification process is illustrated in Fig. 1.

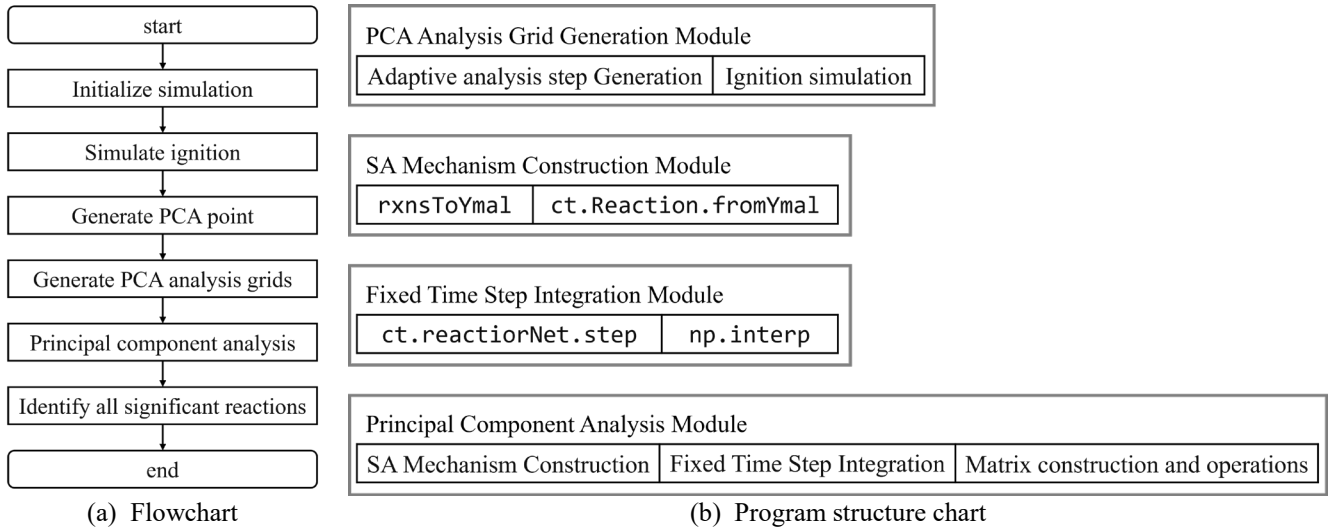


Fig. 1: PCA-based mechanism simplification process

2.2. Mechanism Optimization Method Based on NSGA-III

Constant-pressure premixed combustion can reflect the chemical reaction pathways. Therefore, this optimization focuses on this process. First, simulations of both the detailed and simplified mechanisms are conducted. Then, the

differences between the two results are mathematically formulated. The objective function for this optimization problem is defined as

$$\begin{aligned}
 & \underset{A_k, b_k, E_k \in \mathbb{R}}{\text{minimize}} \quad F_{1,m} + F_{2,m} + F_{3,m} + F_{4,m} \\
 F_{1,m} = & \sum_{i \in I_f} \left(\frac{\int_{\tau_s}^{\tau_e} |x_{i,m} - x_{i,m}^D| dt}{\int_{\tau_s}^{\tau_e} |x_{i,m}^D| dt} \right)^2, \quad F_{2,m} = \sum_{i \in I_p} \left(\frac{\tau_{p,j,m} - \tau_{p,j,m}^D}{\tau_{p,j,m}^D} \right)^2 \\
 F_{3,m} = & \left(\frac{\int_{\tau_s}^{\tau_e} |T_m - T_m^D| dt}{\int_{\tau_s}^{\tau_e} |T_m^D| dt} \right)^2, \quad F_{4,m} = \left(\frac{\tau_{T,m} - \tau_{T,m}^D}{\tau_{T,m}^D} \right)^2
 \end{aligned} \tag{6}$$

where $F_{1,m}, F_{2,m}, F_{3,m}, F_{4,m}$ are parts of the objective function $x_{i,m}$ is the mole fraction of species i over time under operating condition m , $\tau_{p,j,m}$ is the time at which species j reaches its peak value under operating condition m , T_m is the change of temperature with time under operating condition m , $\tau_{T,m}$ is the time when the temperature reaches its peak under operating condition m . The superscript D indicates the detailed mechanism simulation results of the variables. A_k, b_k, E_k are the reaction rate constants of the simplified mechanism, corresponding to the pre-exponential factor, temperature exponent, and activation energy.

NSGA-III requires defining reference directions before optimization. The Riesz s-Energy method is used to generate these reference directions, defining the Riesz s-potential energy in a multi-dimensional space as

$$U(\mathbf{z}^{(i)}, \mathbf{z}^{(j)}) = \frac{1}{\|\mathbf{z}^{(i)} - \mathbf{z}^{(j)}\|^s} \tag{7}$$

where $\mathbf{z}^{(i)}$ and $\mathbf{z}^{(j)}$ are two points in a multi-dimensional space, $\|\mathbf{z}^{(i)} - \mathbf{z}^{(j)}\|^s$ is the Euclidean distance between them raised to the power of s , which is a parameter used to adjust the weight of the distance. Thus, the total potential energy of the system can be obtained as

$$U_T(\mathbf{z}) = \frac{1}{2} \sum_{i=1}^n \sum_{j=1, j \neq i}^n \frac{1}{\|\mathbf{z}^{(i)} - \mathbf{z}^{(j)}\|^s}, \quad \mathbf{z} \in \mathbb{R}^{n \times M} \tag{8}$$

3. Results and Discussion

The mechanism simplification is based on the composition distribution, temperature, and pressure at the nozzle exit of a liquid oxygen-methane rocket engine with an oxidizer-to-fuel ratio of 3.5 and an expansion ratio of 40. Nine simplified operating conditions were established, as shown in Table 1, covering oxygen-rich and fuel-rich conditions within the high-altitude pressure range.

Table 1: PCA simplification operating conditions

Num	Pressure/MPa	Equivalence ration	Initial temperature /K
1	0.26	0.25	1908
2	0.26	1.0	1908
3	0.26	4.0	1908
4	0.026	0.25	1908
5	0.026	1.0	1908
6	0.026	4.0	1908
7	0.0026	0.25	1908

8	0.0026	1.0	1908
9	0.0026	4.0	1908

Ultimately, a simplified reaction mechanism consisting of 25 species and 34 reaction steps was developed. Using simplified mechanism, constant-pressure combustion simulations were performed under different pressures and equivalence ratios, with the results shown in Fig. 2. It can be observed that under low-pressure and oxygen-rich conditions, the simplified mechanism shows significant deviations compared to the GRI 3.0 mechanism, with ignition delay errors exceeding 40%.

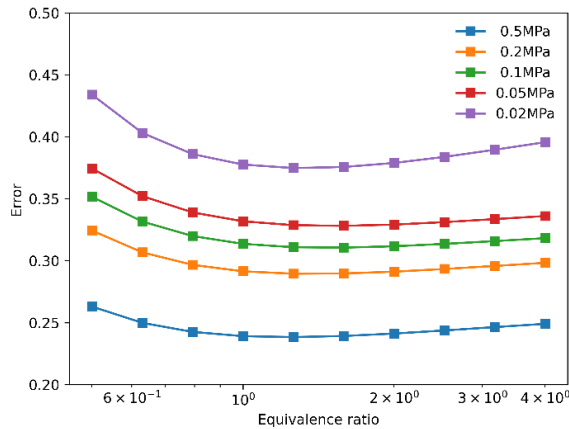


Fig. 2: s25r34 mechanism ignition delay time error

Optimization was conducted under multiple combinations of operating conditions. During the process, it was observed that: Selecting too many operating conditions significantly increases computational costs and slows convergence; Selecting too few operating conditions leads to overfitting, where the optimized mechanism performs well only under the chosen conditions but exhibits large errors in other scenarios. Through iterative adjustments of the optimization scope and operating condition selection, a final set of two pressure conditions and three mixture ratio conditions was chosen, as detailed in Table 2.

Table 2: NSGA-III optimization operating conditions

Num	Pressure/MPa	Equivalence ration	Initial temperature /K
1	0.2	0.5	1908
2	0.2	1.0	1908
3	0.2	2.0	1908
4	0.026	0.5	1908
5	0.026	1.0	1908
6	0.026	2.0	1908

The point with the smallest hypersphere radius on the pareto front was selected to generate the optimized reaction mechanism. Then a zero-dimensional ignition simulation was performed. The results are shown in Figure 3. It can be seen that the ignition delay error is significantly reduced, with the optimization effect being particularly evident under low-pressure and oxygen-rich conditions. The maximum error is reduced to approximately 25%.

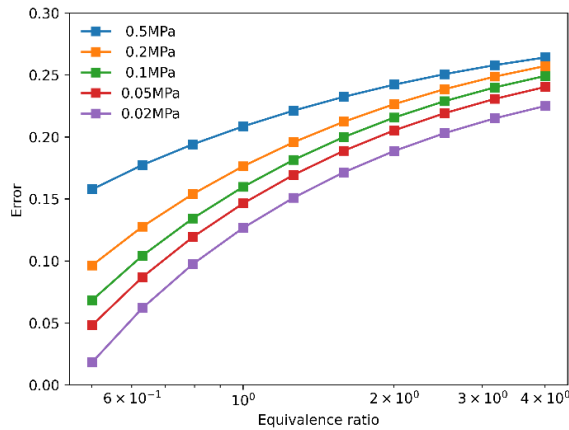
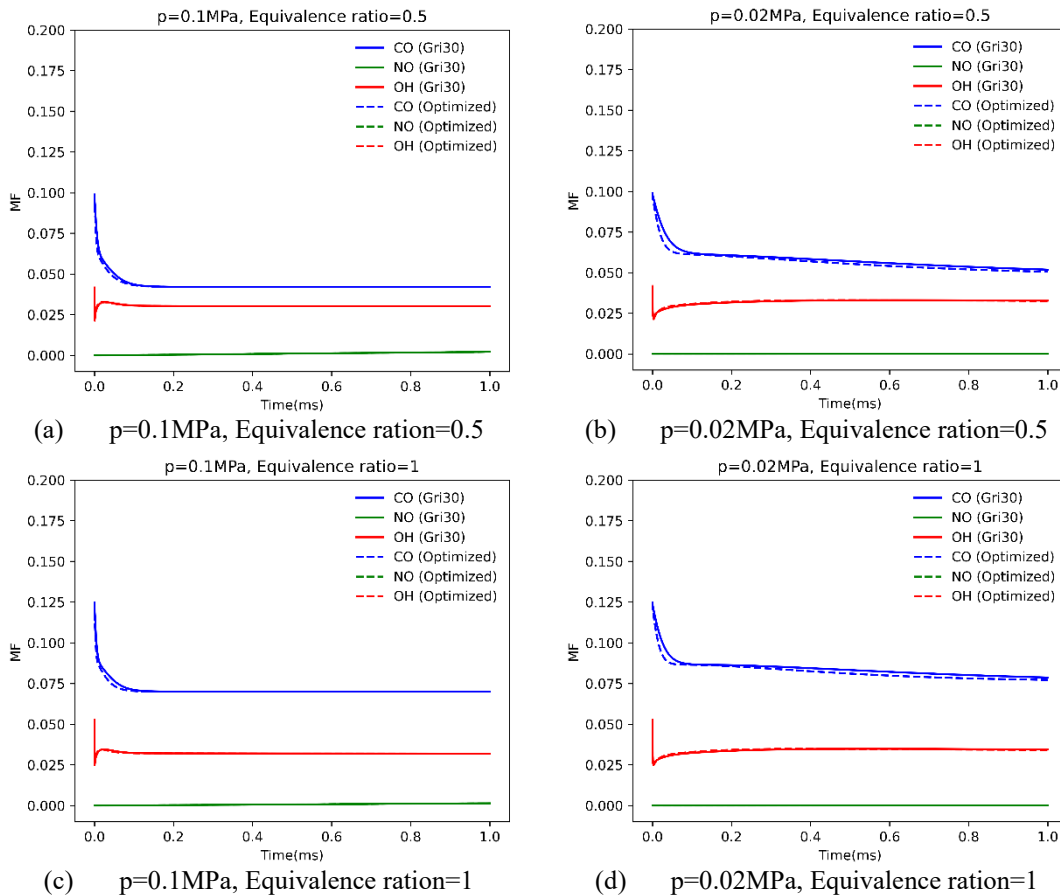


Fig. 3: Optimized mechanism ignition delay time error

Three key reaction products, CO, NO, OH, were selected for analysis. The mole fraction (MF) variation over time for these species, obtained using both the optimized simplified mechanism and the detailed mechanism, is shown in Fig. 4. It can be seen that the temporal evolution of species concentrations in the optimized mechanism closely matches that of the detailed mechanism. Under sea-level conditions ($p = 0.1$ MPa), the species concentration trends align more closely with the detailed mechanism compared to high-altitude conditions ($p = 0.02$ MPa). Overall, the errors introduced by the simplification and optimization process remain within an acceptable range.



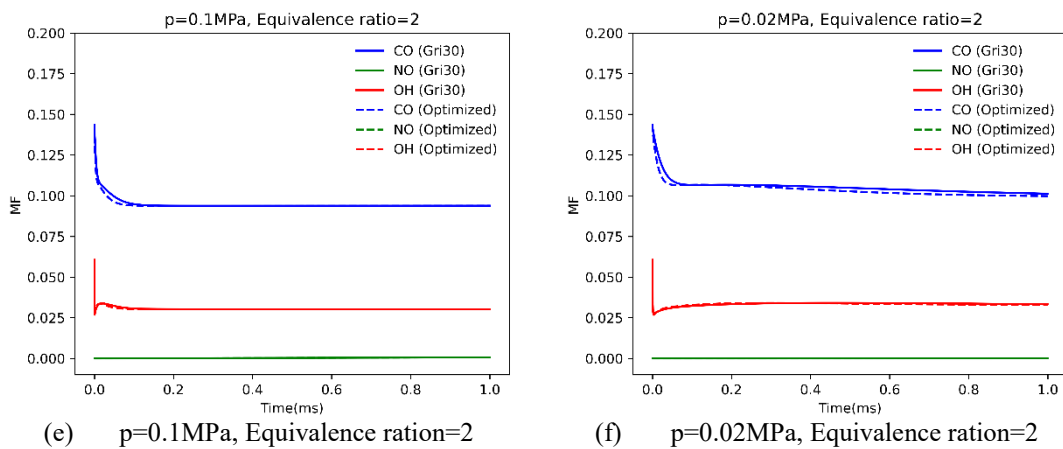


Fig. 4: Temporal evolution of species mole fraction under different conditions

4. Conclusion

This study developed a simplified reaction mechanism for CFD simulations of the liquid oxygen-methane rocket re-entry process, utilizing Principal Component Analysis (PCA) and the NSGA-III optimization algorithm. Based on comparisons with the detailed mechanism, the following conclusions were drawn:

- 1) The GRI 3.0 detailed mechanism was simplified using PCA, resulting in a 25-species, 34-reaction mechanism. The number of species and reactions was significantly reduced. However, the ignition delay error was relatively large, with a maximum error exceeding 40% under low-pressure and oxygen-rich conditions.
- 2) The simplified mechanism was further optimized using NSGA-III. The results show significant improvements, especially in low-pressure and oxygen-rich conditions, with the maximum ignition delay error reduced to approximately 25%.
- 3) By comparing the temporal evolution of three key species between the optimized and detailed mechanisms, the errors introduced by the simplification of the mechanism and the optimisation process are considered to be within acceptable range.

The final optimized simplified mechanism effectively balances computational efficiency and accuracy, significantly reducing computational costs while maintaining sufficient precision. It provides a valuable reference for enhancing CFD simulation efficiency in rocket re-entry process.

References

- [1] B. Weimin, "A review of reusable launch vehicle technology development," *Acta Aeronautica et Astronautica Sinica*, 2023, 44(23): 629555 (in Chinese).
- [2] J.H. Thomas, V.A. Vanessa, R. Shann, C. Charles, S. Richard, C. David Mercer, T. Steven, S.S. Thomas, G. David, O.W. Kwame, K. Steve, S. Gordon, P. Tait, R. Martin "Advancing Supersonic Retro-Propulsion Technology Readiness: Infrared Observations of the SpaceX Falcon 9 First Stage," *AIAA Paper* 2017-5294, 2017.
- [3] E. Tobias, K. Sebastian, D. Etienne, S. Sven, K. Daniel, "A Numerical Study on the Thermal Loads during a Supersonic Rocket Retro-propulsion Maneuver," *AIAA Paper* 2017-4878, 2017.
- [4] E.S. Oran, J.P. Boris, "Numerical simulation of reactive flow," *Cambridge University Press*, 2000.
- [5] D. Sihan, Y. Nanjia, H. Shutao, H. Haodong, "pyMechOpt: A Python toolbox for optimizing of reaction mechanisms," *SoftwareX*, Volume 29, 2025, 102001.
- [6] J.M. Chambers, Y. Bard. "Nonlinear Parameter Estimation," *Technometrics*, 1975, 17(2):271.